Macromolecules

ARTICLE

pubs.acs.org/Macromolecules

Encapsulation Efficiency and Micellar Structure of Solute-Carrying Block Copolymer Nanoparticles

Jeffrey L. Woodhead and Carol K. Hall*

Department of Chemical and Biomolecular Engineering, North Carolina State University, Raleigh, North Carolina 27695-7905, United States

ABSTRACT: We use discontinuous molecular dynamics (DMD) computer simulation to investigate the encapsulation efficiency and micellar structure of solute-carrying block copolymer nanoparticles as a function of packing fraction, polymer volume fraction, solute mole fraction, and the interaction parameters between the hydrophobic head blocks and between the head and the solute. The encapsulation efficiency increases with increasing polymer volume fraction and packing fraction but decreases with increasing head−head interaction strength. The latter is due to an increased tendency for the solute to remain on the micelle surface. We compared two different nanoparticle assembly methods: one in which the solute and copolymer coassociate and the other in which the copolymer micelle is formed before the introduction of solute. The assembly method does not affect the encapsulation efficiency but does affect the solute uptake kinetics. Both head−solute interaction strength and head−head interaction strength affect the density profile of the micelles; increases in the former cause the solute to distribute more evenly throughout the micelle, while increases in the latter cause the solute to concentrate further from the center of the micelle. We explain our results in the context of a model of drug insertion into micelles formulated by Kumar and Prud'homme; as conditions become more conducive to micelle formation, a stronger energy barrier to solute insertion forms which in turn decreases the encapsulation efficiency of the system.

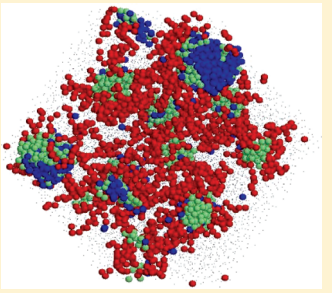

INTRODUCTION

Nanoparticles formed by the micellization of block copolymers in the presence of cancer drugs are now being investigated as a way to reduce the low drug solubility and imprecise targeting associated with standard chemotherapy.[1,2] For example, the ability of micelles formed by PEG-*b*-poly(propylene sulfide) to encapsulate the water-insoluble drug cyclosporin A is the subject of a report by Velluto et al.[3] Encapsulating a drug within a micelle increases the drug's effective solubility in the bloodstream, allowing smaller doses to be delivered with the same effect. Targeting ligands added to the nanoparticle surface increase the likelihood that the drug will be released in the vicinity of cancer cells and prevent them from killing healthy cells.[2] Researchers studying these types of drug delivery systems have, however, reported some problems, most notably with low encapsulation efficiencies and undesirably fast release profiles.[4−7]

The aim of our work is to provide a theoretical framework that describes the assembly of block copolymer micelles in the presence of drug molecules. Motivation for this work is our hope that this will serve as a guide that can assist researchers on the front line to optimize the drug encapsulation efficiency of their systems. Computer simulation can be used to provide this theoretical framework. Although other researchers have used computer simulation, as well as theoretical methods, to study micellization of block copolymers,[8−15] none of them specifically address what occurs when drugs are introduced into a block copolymer system. This is the gap that we seek to fill.

Prud'homme and Kumar formulated a theory of drug encapsulation that describes the free energy necessary to insert a drug into the core of an already-formed block copolymer micelle.[16] They determined that the free energy needed to insert a drug into the core of the micelle increases with the number of drugs in the micelle until the system reaches equilibrium and no more drug can be inserted. Their model describes the case in which micelles form before drug is introduced into the system and hence does not apply to the case considered here in which the micelle-forming block copolymer and the drug are introduced into solution simultaneously.

In a previous study,[17] we modeled drug encapsulation as a solubilization process wherein generalized model solutes are encapsulated in a block copolymer micelle immersed in a solvent. Discontinuous molecular dynamics computer simulations were used to investigate the structural phase behavior of this model copolymer−solute−solvent system to determine (a) the effect of hydrophobic solute particles on the phase behavior of the system and (b) which system variables most affect that phase behavior. We found that the presence of hydrophobic solute particles makes micelles form more easily and that the key variable that determines whether the system encapsulates solute well is the head−solute interaction strength (ε_{hd}). The copolymer/solute/solvent system formed five types of structural phases or morphologies. In three of these phases, all of which occur at low values of ε_{hd}, the solute and copolymers act as coexisting separate systems: micelles may form while the solute remains unaggregated, the solute may aggregate outside the micelles, or the solute may aggregate while the polymers do not. In the other two

Received: December 24, 2010
Revised: May 3, 2011
Published: June 14, 2011

phases, encapsulation occurs, but the manner in which the solute is encapsulated is significantly different. In the first of these phases, which occurs at moderate values of ε_{hd} and at high packing fraction, the solute particles form a large cluster that is surrounded by copolymer. In the second phase, which occurs at high ε_{hd} and all packing fractions, the micelles formed are much smaller and the solute is evenly dispersed among them. This phase, which we referred to as "micelles encapsulating dispersed solute", is characteristic of the kind of drug encapsulation sought in the lab.

In this paper we focus in on the encapsulation of drug (solute) molecules in the "micelles encapsulating dispersed solute" phase described in our previous paper on copolymer/solute/solvent systems. Discontinuous molecular dynamics simulations are applied to this three-component system (copolymer, drug, solvent) with the copolymers modeled as square-well chains of length 12 and the drugs modeled as square-well spheres. The dependence of the encapsulation efficiency and micelle density profile on the packing fraction, polymer volume fraction, head−solute interaction strength, head−head interaction strength, and solute mole fraction is analyzed. Our results are compared to the predictions of the Prud'homme−Kumar model so as to determine the degree to which their model can be applied to systems where copolymer and solute coassociate. We also model the encapsulation efficiency of a system where the micelles form before the solute is introduced in order to compare the encapsulation efficiency and kinetics of these two methods of nanoparticle construction.

Highlights of our results include the following. Increasing the system packing fraction increases the amount of solute encapsulated and decreases the amount of solute that remains on the micelle surface. Increasing the polymer volume fraction increases the encapsulation efficiency of the system as expected, but this effect saturates at high polymer volume fraction. The encapsulation efficiency of the system depends quite sensitively on the values of the interaction parameters, especially the head−head interaction strength. Increases in the head−head interaction strength strongly impede encapsulation ability by forcing drug particles to remain on the micelle surface. An increase in solute mole fraction changes the encapsulation efficiency at high values of head−head interaction strength, but not at lower values of head−head interaction strength. At the higher head−head interactions, the system of micelles has a fixed carrying capacity; once that capacity is exceeded, the micelles start to encapsulate large clusters of solutes. Analysis of the density profiles of the solute-encapsulating micelles indicates that increases in head−solute interaction strength lead the solute and head blocks to be distributed more evenly throughout the core of the micelle, while an increase in head−head interaction strength causes micelles to become smaller and solute to shift from the center of the micelle to the outside. There is surprisingly little difference in encapsulation efficiency between the case in which solutes are introduced to a preformed system of micelles and the case in which solutes and copolymer coassociate. There is, however, a difference in the kinetics of encapsulation between the two nanoparticle assembly methods at high values of the head−head interaction strength. Solute uptake for the case in which micelles coassociate with copolymer is faster than in the case in which micelles are preformed; however, both cases result in the same overall encapsulation efficiency. Our results can be interpreted in terms of the model of Kumar and Prud'homme; as conditions become more conducive to micelle formation, a stronger energy barrier to solute insertion forms, which in turn decreases the encapsulation efficiency of the system.

Table 1. Matrix of Interaction Parameters

	ε_{ij}			
	head	tail	solvent	solute
head	ε_{hh}	0	0	ε_{hd}
tail		0.4	0.45	0
solvent			0	0
solute				1.0

METHODS

As in our previous research, we used discontinuous molecular dynamics (DMD) simulation. In DMD, particle interactions are modeled by square-well potentials instead of by Lennard-Jones potentials as in traditional molecular dynamics simulations, eliminating the need to numerically integrate Newton's laws at discrete time steps. This saves computational time, making DMD well suited to modeling large systems over long time periods.[18] Since the encapsulation of solute within micelles occurs over a long time and requires a large system to investigate properly, DMD is ideal for our purposes.

The model used in this paper is the same model as that employed in our previous paper on micelle formation in the presence of solutes.[17] The copolymer is modeled as a chain of 12 square-well spheres with four solvent-phobic head (H) spheres and eight solvent-philic tail (T) spheres, represented symbolically as H_4T_8. Solute particles (D) are modeled as square-well spheres. Solvent molecules (S) are modeled as single spheres with square-well interactions with head and tail spheres and hard-sphere interactions with other solvent spheres. All spheres have a diameter of $\sigma = 1.0$. The depth of the square well potential between two particles, ε_{ij}, is a measure of the strength of the interaction between them. The values for the interaction energies in the model are given in Table 1; the head−solute, ε_{hd}, and head−head interaction, ε_{hh}, strengths are varied.

Other system variables are as follows. The packing fraction, which is related to the density of the system, is defined as $\eta = 6N\sigma^3/\pi V$, where N is the number of spheres in the system and V is the volume of the simulation box. The polymer volume fraction is the number of polymer spheres divided by the total number of spheres and is related to the polymer mole fraction, x_{pol}, as follows:

$$\varphi = \frac{(N_{pol} + N_d + N_{sol})R}{N_{pol}R + N_d + N_{sol}} x_{pol}$$

where R is the length of the copolymer and N_i is the number of spheres of component i. The reduced temperature is defined as $T^* = kT/\varepsilon^*$, where k is Boltzmann's constant and ε^* is a reference interaction energy.

We have maintained our system variables so that they fall in the "micelles encapsulating dispersed solute" portion of the phase diagram from our previous research.[17] In this phase, the copolymers form numerous moderately sized micelles with the solute distributed evenly among them. The values for the variables are packing fraction $\eta = 0.3$, polymer volume fraction $\varphi = 0.174$, and solute mole fraction of $x_d = 0.0174$. The

dx.doi.org/10.1021/ma102938g |Macromolecules 2011, 44, 5443–5451

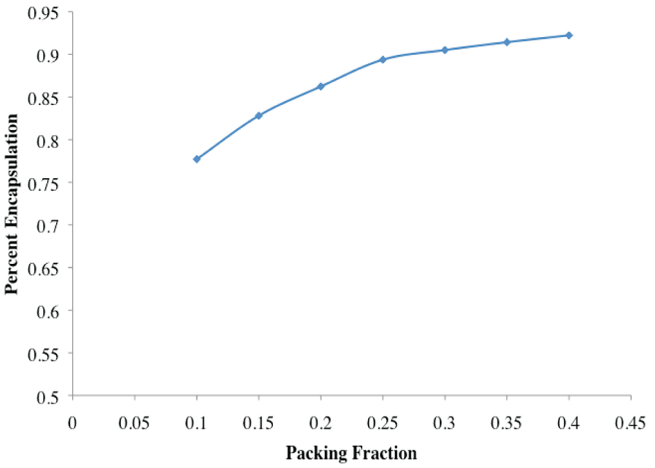

Figure 1. Percent of solute particles encapsulated at different system packing fractions. $\varepsilon_{hh} = 1.0$, $\varepsilon_{hd} = 1.2$, $\varphi = 0.174$.

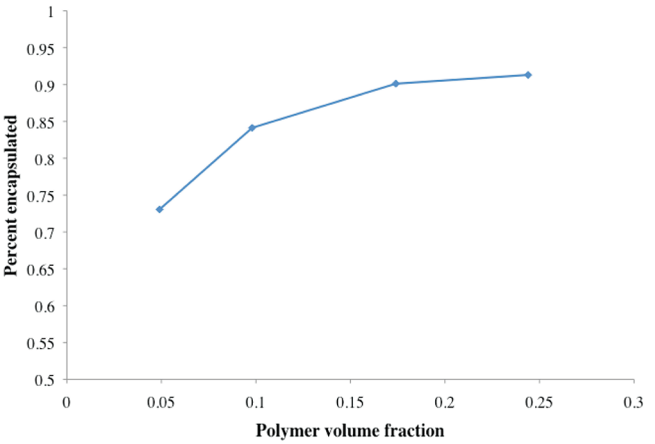

Figure 2. Percent of solute particles encapsulated at varying polymer volume fraction. $\varepsilon_{hh} = 1.0$, $\varepsilon_{hd} = 1.2$, $\eta = 0.3$.

head−solute interaction strength (ε_{hd}) and head−head interaction strength (ε_{hh}) are varied. The reduced temperature T^* is held constant at 1.0 after a steady cooling from an initial temperature of $T^* = 4.0$; this is done to ensure that the system is well-mixed and to prevent it from becoming trapped in a local energy minimum. The temperature is kept constant through the use of the Anderson thermostat wherein "ghost particles" collide with system particles regularly in order to keep the velocities of the particles consistent with the Boltzmann distribution at a given temperature.[19,20] The solute volume fraction and the polymer volume fraction are higher than the values generally used in experiments. These values were chosen for computational convenience: simulations of systems with smaller, more-realistic values take much too long to equilibrate. We do not expect that the high volume fraction and mole fraction used in our research will have a significant qualitative effect on our results regarding other variables.

DMD simulations are performed in the canonical ensemble (constant N, V, T). The number of particles in the system is held constant at 13 683, with 2400 copolymer spheres configured in 200 H_4T_8 chains, 200 solute spheres, and 11 083 solvent spheres. The number of copolymers in the system changes when the polymer volume fraction changes; in order to hold the drug mole fraction constant, we must change the number of solvent spheres in the system when this occurs.

Each data point requires an equilibration run and a production (data collection) run. In an equilibration run, the initial configuration is a system of randomly placed H_4T_8 chains in random coil conformations, solvent molecules, and drug molecules. The simulation proceeds for a total of 100 000 reduced time units (roughly 4×10^9 DMD events) though this depends upon the system size and packing fraction. The final configuration is then used as the initial configuration for a 5000 time unit production run during which the number of encapsulated drugs in each system and the density profile of each micelle is recorded.

The encapsulation efficiency and related terms are defined in the following way. A solute particle is defined to be "encapsulated" when it is within the square well of a head sphere that is part of a micelle containing six or more copolymers but is not on the surface of the micelle, meaning it is not also within the square well of a tail sphere. A solute particle is defined to be "surface bound" when it within the square well of a tail sphere that is part of a micelle containing six or more copolymers and also within the square well of a head sphere. Surface-bound drug molecules have been implicated in poor release patterns of drug-carrying nanoparticles.[4,19,20] We restrict our attention to micelles with copolymer aggregation number of 6 or greater because aggregates with aggregation number less than 6 have also been ignored by previous researchers.[21,22] We define encapsulation efficiency as the percentage of solute spheres in the system that are encapsulated.

The density profile of any component across a solute/copolymer aggregate is determined by finding the aggregate's center of mass, calculating the number of component spheres in a spherical shell at each distance from the center of mass and then dividing by the volume of the shell.

RESULTS

We first investigated the effect that variations in the packing fraction and polymer volume fraction had on the encapsulation efficiency of the system. Figure 1 shows the percentage of solutes encapsulated as a function of the system packing fraction at $\varepsilon_{hd} = 1.2$, $\varepsilon_{hh} = 1.0$, and $\varphi = 0.174$. As the graph shows, the encapsulation efficiency of the system increases moderately as the packing fraction increases. This is due to the fact that increases in packing fraction make it harder for micelles to form. As the Kumar−Prud'homme model suggests,[16] the harder it is for micelles to form, the lower the energy barrier to solute entry into the micelle, thus enhancing the amount of solute encapsulated within the micelle. We will explore this phenomenon in more depth shortly.

Figure 2, which shows encapsulation efficiency as a function of the polymer volume fraction at $\varepsilon_{hd} = 1.2$, $\varepsilon_{hh} = 1.0$, and $\eta = 0.3$, demonstrates that increases in polymer volume fraction increase the encapsulation efficiency of the system. The existence of more polymer in the system leads to more micelles and thus more encapsulation. The effect of polymer volume fraction on encapsulation efficiency is not linear but instead levels off at φ greater than 0.175. This is likely due to the fact that at the higher polymer volume fractions we are left with excess polymer.

It is interesting to examine how the chemical nature of the copolymers and solutes affects the encapsulation efficiency. We use the interaction parameters as a proxy for (or measure of) the type of copolymer or drug molecule considered, focusing on the head−head interaction strength, ε_{hh}, and the head−solute

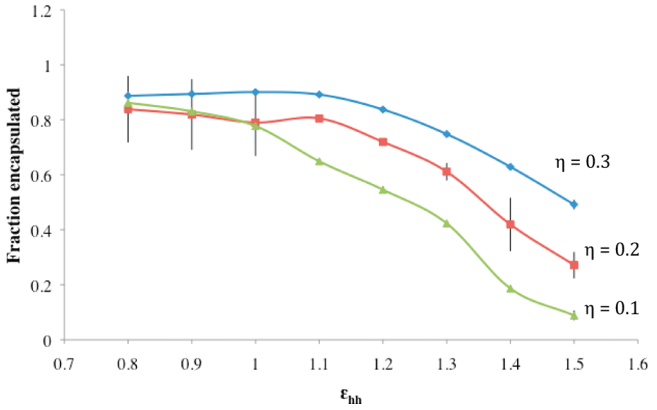

Figure 3. Fraction of solute particles encapsulated at varying head—head interaction strength. $\varepsilon_{hd} = 1.2$, $\varphi = 0.174$.

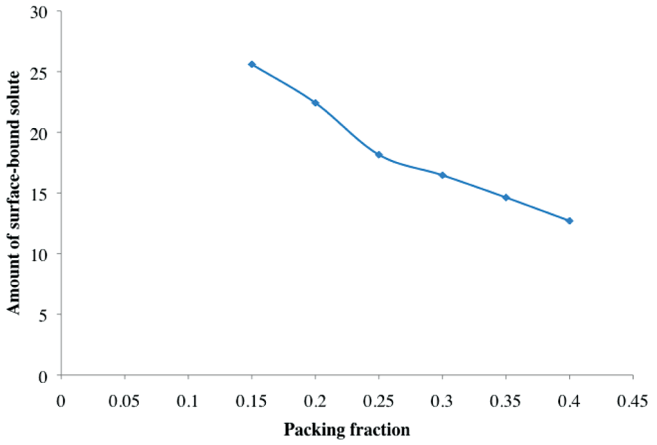

Figure 4. Number of surface-bound solutes versus packing fraction at $\varepsilon_{hh} = 1.0$, $\varepsilon_{hd} = 1.2$, and $\varphi = 0.174$.

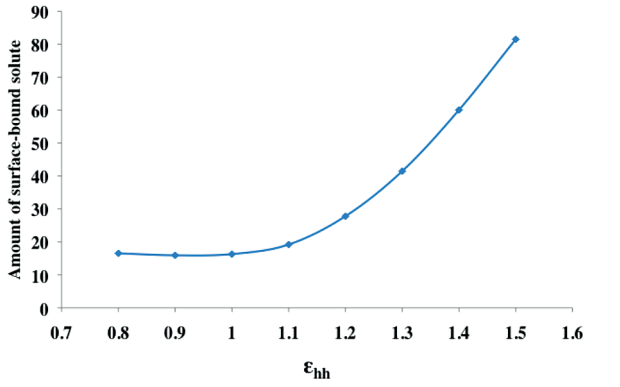

Figure 5. Number of surface-bound solute particles at varying head—head interaction strength. $\varepsilon_{hd} = 1.2$, $\eta = 0.3$, $\varphi = 0.174$.

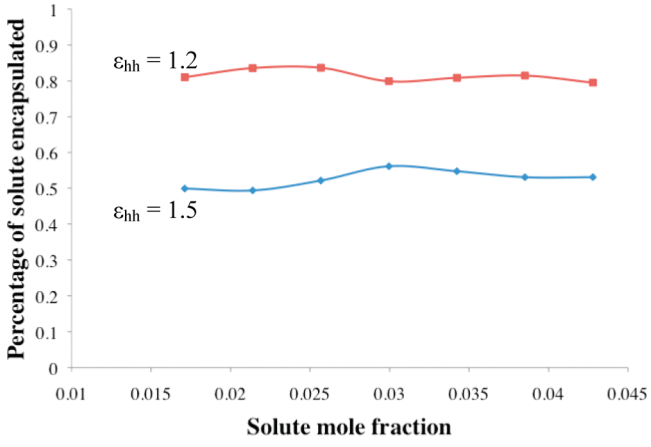

Figure 6. Percentage of solute encapsulated at varying solute mole fraction, $\varepsilon_{hd} = 1.2$, $\eta = 0.3$, $\varphi = 0.174$, and $\varepsilon_{hh} = 1.2$ and 1.5.

interaction strength, ε_{hd}. While determining specific values of ε_{hh} and ε_{hd} are beyond the scope of this paper, our previous paper contains a discussion of how these parameters relate to the type of polymer and drug in the system and how one might calculate these parameters for a particular copolymer—solute pair.[17] A change in ε_{hh} is indicative of a change in copolymer hydrophobicity—a higher value of ε_{hh} means that the head block of the copolymer is more hydrophobic. Meanwhile, a change in ε_{hd} is indicative of increased or decreased affinity of the polymer head for the solute.

Figure 3 shows how the encapsulation efficiency (percentage of solute encapsulated) at $\varphi = 0.174$ and $\varepsilon_{hd} = 1.2$ varies with ε_{hh} at three different packing fractions: $\eta = 0.1$, 0.2, and 0.3. We examined values of ε_{hh} from 0.8 to 1.5; lower values of ε_{hh} did not result in micelle formation. At $\eta = 0.3$, the encapsulation efficiency is constant at nearly 90% as ε_{hh} increases from 0.8 to 1.1 but declines steeply thereafter, reaching an encapsulation efficiency of less than 50% at $\varepsilon_{hh} = 1.5$. Thus, increasing the head blocks' self-affinity hinders the encapsulation efficiency of the system. A plausible explanation for this is that the attraction between the head blocks creates a high energetic barrier to entry into the micelle core, so that solute particles that would normally enter the micelle core get trapped on the surface. Thus, even though the micelles form more easily as ε_{hh} increases, they form so tightly that they lock drugs out.

Figure 3 also shows how the packing fraction influences the dependence of encapsulation efficiency on ε_{hh}. At low ε_{hh}, the packing fraction has little effect on the encapsulation efficiency of the system, and the three curves for $\eta = 0.1$, 0.2, and 0.3 overlap. However, as ε_{hh} increases, the curves separate; the encapsulation-diminishing effect of increasing ε_{hh} is far more pronounced at the lower packing fractions. At the highest value of ε_{hh}, the difference is stark; at $\eta = 0.3$, the system still encapsulates over half the solute in the system, while at $\eta = 0.1$, the system encapsulates roughly 10% of the available solute. These results are consistent with our earlier results that show that encapsulation efficiency increases as packing fraction increases.

The connection between the conditions that encourage the formation of micelles and the likelihood that a solute will be surface-bound can be seen in Figures 4 and 5. Figure 4 shows the number of surface bound solutes as a function of packing fraction when $\varepsilon_{hh} = 1.0$, $\varepsilon_{hd} = 1.2$, and $\varphi = 0.174$. The number of surface-bound solutes decreases as packing fraction increases. Figure 5 shows the number of surface bound solutes as a function of the head—head interaction strength, ε_{hh}, at $\eta = 0.3$, $\varphi = 0.174$, and $\varepsilon_{hd} = 1.2$. As head—head interaction strength increases, more solute becomes bound to the surface of the micelle. Since both increasing the head—head interaction strength and decreasing the packing fraction make micelle formation easier, this reveals that increasing the tendency of copolymers to form micelles increases

dx.doi.org/10.1021/ma102938g |*Macromolecules* 2011, 44, 5443–5451

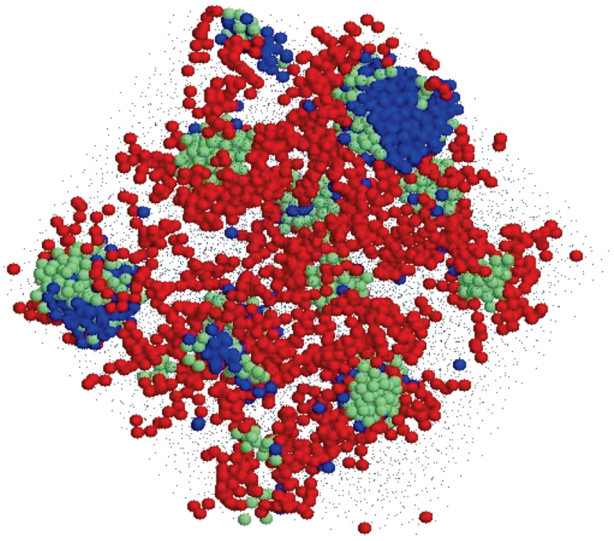

Figure 7. Snapshot of the system at equilibrium for $\varepsilon_{hd} = 1.2$, $\varepsilon_{hh} = 1.5$, $\eta = 0.3$, $\varphi = 0.174$, and $x_d = 0.0428$. Note the large drug aggregate in the system.

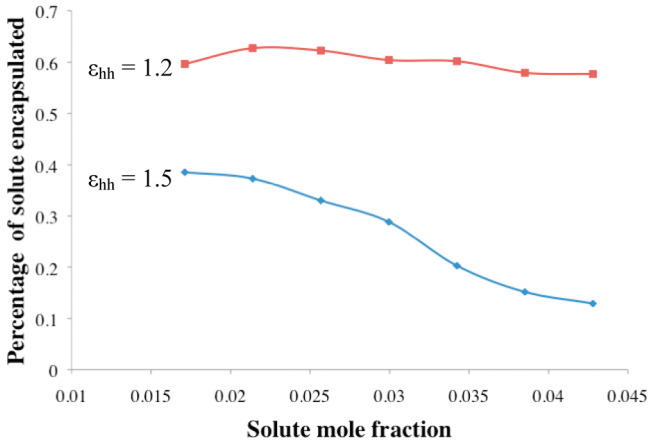

Figure 8. Percentage of solute encapsulated after subtracting the size of the largest solute aggregate from the total number of solutes encapsulated. $\varepsilon_{hd} = 1.2$, $\eta = 0.3$, $\varphi = 0.174$.

the number of solute particles on the surface of the micelle while decreasing the amount of solute encapsulated within the micelle.

We also investigate the dependence of the encapsulation efficiency on the mole fraction of solute. Figure 6 shows the percentage of solutes encapsulated as a function of solute mole fraction at $\varphi = 0.174$, $\eta = 0.3$, and $\varepsilon_{hh} = \varepsilon_{hd} = 1.2$. The percentage of solutes encapsulated is the same at all values of the solute mole fraction investigated. Similar results are seen when ε_{hh} is increased to 1.5 as is also indicated in Figure 6; i.e., there appears to be no change in encapsulation efficiency as the solute mole fraction increases.

The conclusion reached above, that encapsulation efficiency is insensitive to solute mole fraction, is not entirely correct at higher head−head interaction strength ($\varepsilon_{hh} = 1.5$). A fuller picture of the phenomena can be obtained by distinguishing between encapsulation of a single large aggregate of solutes (a solute cluster) and encapsulation of solutes that are dispersed throughout all of the micelles in the system. (The latter case corresponds to the most desirable type of encapsulation as is discussed in our previous paper.) Figure 7 shows a snapshot of the system after equilibration at $\varphi = 0.174$, $\eta = 0.3$, $\varepsilon_{hh} = 1.5$, $\varepsilon_{hd} = 1.2$, and $x_d = 0.0423$, which suggests that both types of encapsulation are occurring at these conditions. To discount the presence of the large cluster, we have in Figure 8 subtracted the largest solute cluster from the average to display the percentage of solutes at $\varepsilon_{hh} = 1.2$ and 1.5 that are "nicely encapsulated" versus solute mole fraction. By "nicely encapsulated", we mean that the solutes are dispersed throughout the micelles in the system. At the lower head−head interaction strength this new measure of encapsulation efficiency remains constant throughout the range of solute mole fractions tested, but at the high head−head interaction strength, it decreases significantly as more solute is added to the system. Thus, at lower head−head interaction strength, encapsulated solute is dispersed throughout the range of x_d tested, but at the higher head−head interaction strength solute clusters begin to be encapsulated as x_d increases. We conclude that at higher values of ε_{hh} a system of micelles has a fixed carrying capacity and that once that capacity is exceeded the micelles will encapsulate large solute clusters.

It is of interest to relate our findings to the theory of drug encapsulation in previously formed micelles introduced by Kumar and Prud'homme. They derive an expression for the change in the surface energy of a micelle when solute is added to the micelle core and discuss how this energy barrier is perturbed by the encapsulation of additional solutes. As the drug loading increases, the free energy required to load a drug into the particle increases until an equilibrium solute loading value is reached. After this equilibrium value is reached, the drug particles do not possess the energy required to enter the micelle core, and loading stops.[16] This theory can be used to explain the results of our simulations. In our simulations, the amount of surface-bound solute increases as encapsulation becomes less likely. Solute particles become stranded on the micelle surface; a plausible explanation for this is that the solute particles that are attempting to enter the micelle core lack the energy to do so. Furthermore, our results show that as the ease of forming micelles increases, encapsulation of solute becomes less likely; this implies that the energy barrier to solute entry grows stronger when micelle formation becomes more favored. This is why changes in system variables that make micelle formation easier—increasing η and increasing ε_{hh}—decrease the encapsulation efficiency of the system while increasing the amount of solute on the micelle surface.

Furthermore, the strength of this apparent energy barrier influences the behavior of the system as more solute is added. As shown in Figure 8, the carrying capacity for the micelles at high head−head interaction strength ($\varepsilon_{hh} = 1.5$) is reached at a relatively low solute mole fraction but is not reached in the range of solute mole fractions investigated at lower head−head interaction strength ($\varepsilon_{hh} = 1.2$). These results are what we would expect to see if the energy barrier to solute insertion grew stronger as the head−head interaction strength increased. The strong energy barrier present at high ε_{hh} limits the amount of drug that could be encapsulated by the system, leading to a system with a low carrying capacity. Meanwhile, the weaker energy barrier present at lower ε_{hh} would not prevent solute from being encapsulated by the system, thus producing a system with a much higher carrying capacity.

It is of interest to see how the nanoparticle assembly method —coassociation of micelles and solute or introduction of solute into preformed micelles—affects the encapsulation efficiency. The simulations described in Figure 3 at $\eta = 0.3$ were rerun for

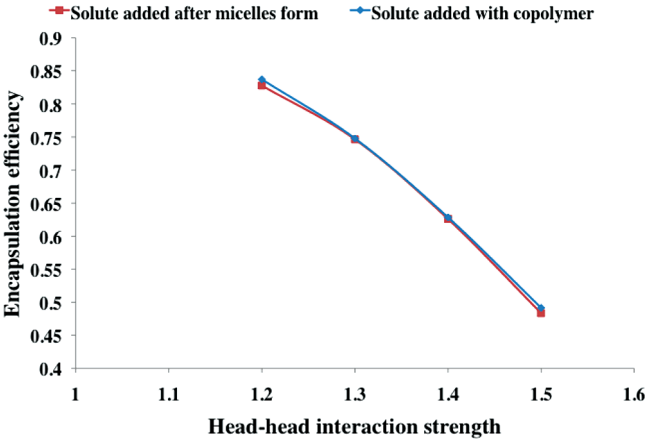

Figure 9. Encapsulation efficiency at various values of ε_{hh} for two different nanoparticle assembly schemes. $\varepsilon_{hd} = 1.2$, $\eta = 0.3$, $\varphi = 0.174$.

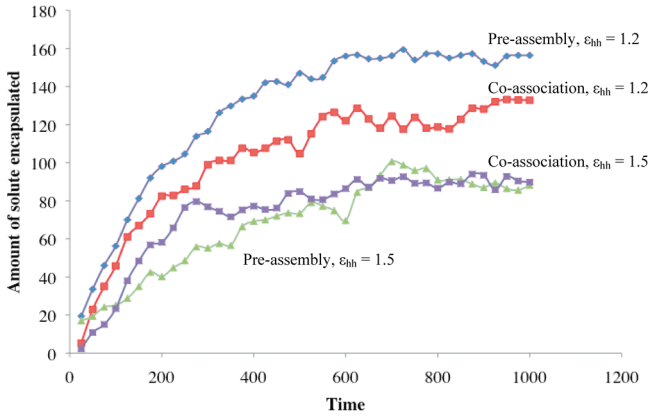

Figure 10. Amount of solute encapsulated versus time for two different methods of nanoparticle assembly (preassembled micelles and coassociation) at two different values of ε_{hh}. Blue: preassembly, $\varepsilon_{hh} = 1.2$. Red: coassociation, $\varepsilon_{hh} = 1.2$. Green: preassembly, $\varepsilon_{hh} = 1.5$. Purple: coassociation, $\varepsilon_{hh} = 1.5$. $\varepsilon_{hd} = 1.2$, $\eta = 0.3$, and $\varphi = 0.174$.

the case in which solutes were added to a system of preformed micelles at $\varphi = 0.174$ and $\varepsilon_{hd} = 1.2$. A solute-free system of H_4T_8 molecules in an initially random configuration was allowed to equilibrate for 100 000 reduced time units, resulting in the formation of micelles. Solutes were then introduced, and the resulting system was equilibrated for another 100 000 reduced time units. Figure 9 compares the encapsulation efficiency as a function of ε_{hh} in both cases. We can see that as we vary ε_{hh}, there is essentially no difference between the case where solute is loaded with the copolymer and the case in which the solute is loaded after micellization. This shows that the strength of the energy barrier does not depend on the method of nanoparticle assembly, and the encapsulation efficiency at which the barrier becomes too difficult for solute to overcome is determined thermodynamically, as Kumar and Prud'homme predicted.

We also compared the solute uptake kinetics for the two nanoparticle assembly methods. Figure 10 shows the amount of solute encapsulated in micelles at $\varepsilon_{hd} = 1.2$, $\eta = 0.3$, and $\varphi = 0.174$ for both preassembled micelles and coassociation over the first 1000 reduced time units for $\varepsilon_{hh} = 1.2$ and $\varepsilon_{hh} = 1.5$. At $\varepsilon_{hh} = 1.2$, the initial slopes of the curves for both assembly methods are the same, meaning that the initial rate of uptake into micelles does not depend strongly on the construction method. At $\varepsilon_{hh} = 1.5$, however, there is a marked difference in the initial uptake rate. For the first 300 reduced time units, micelle uptake into preassembled micelles is significantly slower than encapsulation by coassociation.

We also investigate the manner in which the uptake kinetics of the two assembly methods changes when ε_{hh} is increased. In the coassociation case, the rate of solute uptake is roughly the same for both values of ε_{hh} until about 300 reduced time units. At this point, the encapsulation of solute slows down at both values of ε_{hh} until the peak equilibrium value is reached (which, at the lower value of ε_{hh}, does not occur within the time frame represented in this graph). By contrast, the rate of uptake in the preassembled micelle case is significantly faster at $\varepsilon_{hh} = 1.2$ than it is at $\varepsilon_{hh} = 1.5$. Furthermore, both reach their equilibrium encapsulation efficiency at about 700 reduced time units.

These kinetic phenomena can be explained by the presence of an energy barrier to solute uptake in micelles that is stronger in systems where micelles form more easily. Solute uptake into a preassembled micelle at $\varepsilon_{hh} = 1.2$ is faster than at $\varepsilon_{hh} = 1.5$ because micelles form less easily at lower ε_{hh}, leading to a weaker energy barrier to entry into the empty micelle at the lower ε_{hh}. Meanwhile, in the coassociation case, the energy barrier to uptake does not exist initially because the micelles do not exist initially. Therefore, the initial rate of uptake is similar at both values of ε_{hh}, and the rate of uptake changes only as micelles form with already-encapsulated solute inside.

We can gain useful information from looking at the density profiles of the solute-encapsulating micelles. A density profile is a plot of the concentration of a particular type of sphere (head, tail, solute, or solvent) as a function of the sphere's distance from the aggregate's center of mass. Figure 11 shows the density profiles of the micelles at packing fractions $\eta = 0.15$, 0.3, and 0.4 when at $\varepsilon_{hd} = 1.2$, $\varepsilon_{hh} = 1.0$, and $\varphi = 0.174$. The solute density profile contains a sharp peak near the center of the micelle, demonstrating the existence of a tightly packed core of solute spheres. The head profile contains a broader, lower peak that reaches its maximum outside the drug peak; this means that the tightly packed core of solute is surrounded by a less-tightly packed layer of copolymer. The tail profile contains a low peak well beyond the head peak. As can be seen from Figure 11, as we increase the packing fraction there is little change in the profiles; the peak heights and location do not change much, and the radius of the micelle—determined by the crossover point between head and tail—remains the same. This is surprising because as the system compresses, one would expect the size of the micelles to decrease and the density of particles within the micelles to increase. This suggests that although the system is being compressed, it is compressed in a manner that pushes solvent spheres closer to one another and that such compression does not affect the micelles much. This could explain why encapsulation efficiency appears to not be affected by packing fraction, as well as why packing fraction does not change the phase behavior of the system at high ε_{hd} as determined in our previous paper.

We also looked at how the density profiles of micelles change as ε_{hd} increases—the density profiles at $\varepsilon_{hd} = 1.1$, 1.3, 1.4, and 1.5 when $\varepsilon_{hh} = 1.0$, $\eta = 0.3$, and $\varphi = 0.174$ are shown in Figure 12. As we can see, at the lower values of ε_{hd} (1.1−1.3), the profile suggests the existence of a well-defined core of solute surrounded by a well-defined layer of block copolymer head. However, as ε_{hd} increases, the head peak broadens to develop a more pronounced

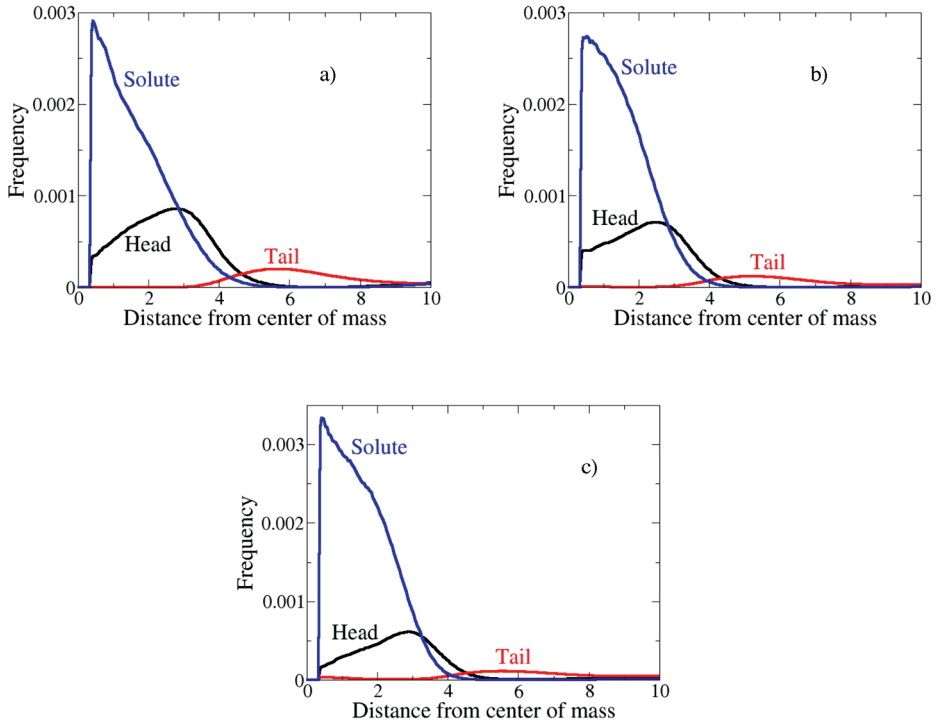

Figure 11. Density profiles for systems at (a) $\eta = 0.15$, (b) $\eta = 0.3$, and (c) $\eta = 0.4$. Solute is in green, head is in black, and tail is in blue. $\varepsilon_{hh} = 1.0$, $\varepsilon_{hd} = 1.2$, $\varphi = 0.174$.

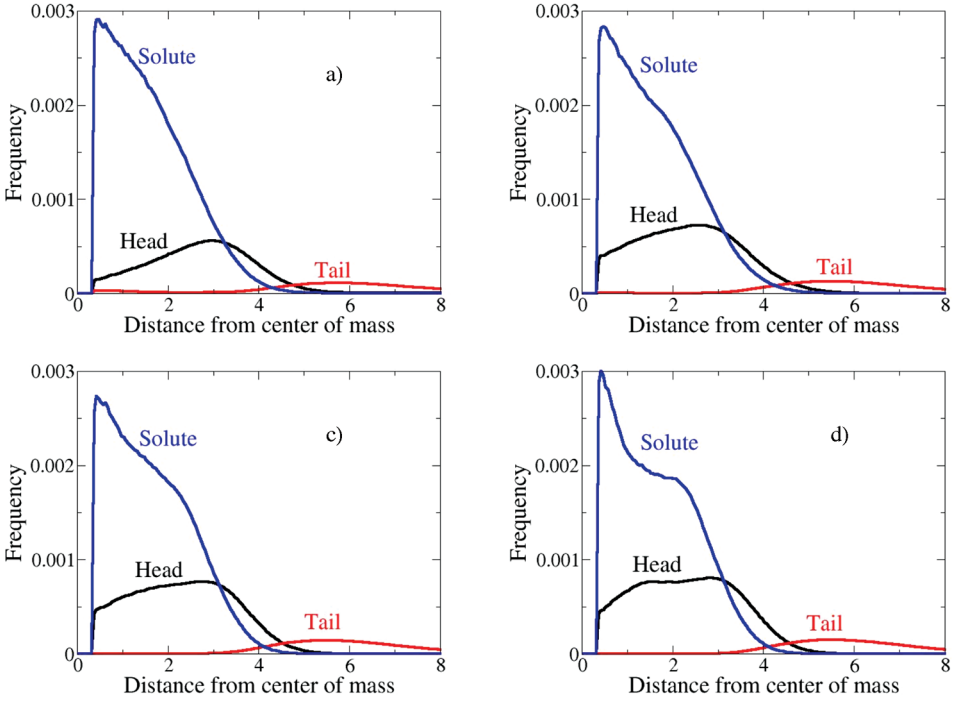

Figure 12. Density profiles for systems at (a) $\varepsilon_{hd} = 1.1$, (b) $\varepsilon_{hd} = 1.3$, (c) $\varepsilon_{hd} = 1.4$, and (d) $\varepsilon_{hd} = 1.5$. $\varepsilon_{hh} = 1.0$, $\eta = 0.3$, $\varphi = 0.174$.

inner layer and the solute broadens to develop a second outer layer. This shows that solute is distributed more evenly throughout the micelles as ε_{hd} increases and that block copolymer head blocks are beginning to unfold themselves toward the center of the micelle.

Figure 13 shows the density profiles of the micelles at $\varepsilon_{hh} = 1.2$, 1.3, 1.4, and 1.5 when $\varepsilon_{hd} = 1.2$, $\eta = 0.1$, and $\varphi = 0.174$. The first interesting thing to notice is that the micelles appear to get smaller in size as ε_{hh} increases; that is, the point at which the head and tail curves cross moves closer to the center of mass of the

dx.doi.org/10.1021/ma102938g |*Macromolecules* 2011, 44, 5443–5451

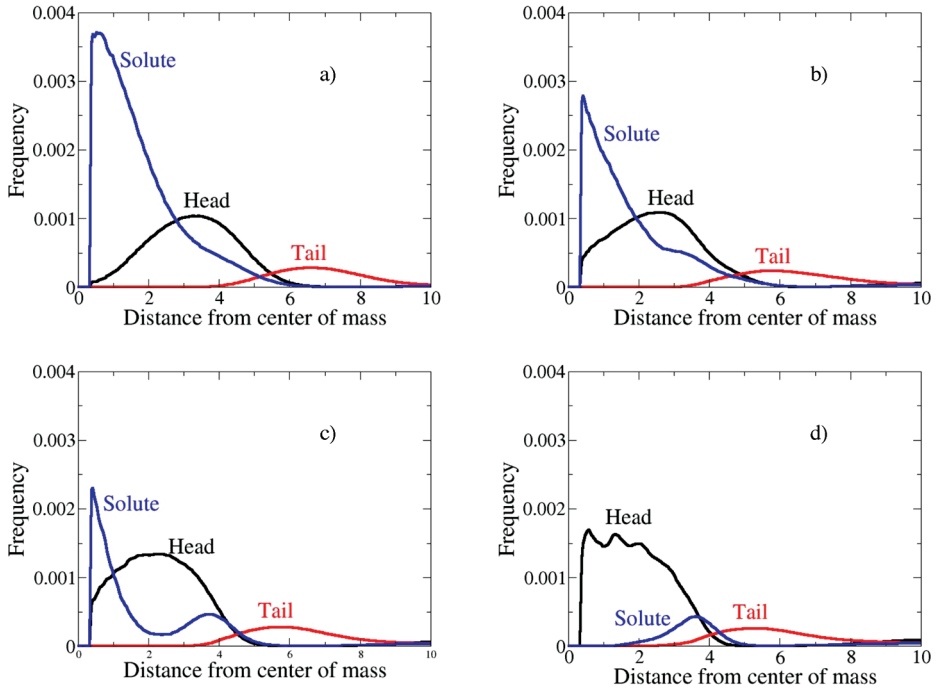

Figure 13. Density profiles for systems at (a) ε_{hh} = 1.2, (b) ε_{hh} = 1.3, (c) ε_{hh} = 1.4, and (d) ε_{hh} = 1.5. ε_{hd} = 1.2, η = 0.1, φ = 0.174.

micelle. The second is that the head and solute peaks exchange places over the range of values of ε_{hh} investigated. As ε_{hh} increases, the head peak becomes larger and moves toward the center while the solute peak shrinks and moves toward the outside. At the lowest value of ε_{hh}, 0.8, there is a core of solute surrounded by a layer of head spheres; at ε_{hh} = 1.5, this has been reversed, so that there is a core of head spheres surrounded by a layer of solute spheres. The changes in the internal structure of the micelle−solute aggregates as ε_{hh} increases demonstrate the stronger energy barrier to solute uptake that exists at higher values of ε_{hh}. The fact that the micelles get smaller as ε_{hh} increases, combined with the fact that the head peak grows in amplitude as ε_{hh} increases, shows that the more hydrophobic copolymer head blocks are forming a tighter structure that is more difficult for solute to penetrate.

CONCLUSIONS

In this study we used computer simulation to investigate the effect of packing fraction, polymer volume fraction, head−head interaction strength, and head−solute interaction strength on the solute encapsulation behavior of a copolymer−solute−solvent system. Increasing the packing fraction of the system mildly decreased its encapsulation efficiency, while increasing the polymer volume fraction increased the system's encapsulation efficiency until a maximum encapsulation efficiency was reached. The head−solute interaction strength does not have a substantial effect on the encapsulation efficiency of the system, but the head−head interaction strength does. Increasing the head−head interaction strength decreases the encapsulation efficiency of the system significantly, and it does so by forcing drugs to settle on the surface of the micelle instead of becoming incorporated into the micelle core.

We also compared the encapsulation efficiency and kinetics of the system for two different nanoparticle assembly methods: one in which empty micelles were preassembled and then loaded with solute and one in which solute and copolymer coassociate. We found no difference in the equilibrium encapsulation efficiencies for the two assembly methods; however, the solute uptake kinetics of the two assembly methods are significantly different, especially at higher values of the head−head interaction strength. Furthermore, the initial speed of uptake into preassembled micelles is strongly dependent on ε_{hh}, while the initial speed of solubilization as copolymer and solute coassociate changes little with ε_{hh}.

We also described how the internal structures of the micelles as measured by the density profile changes as packing fraction as well as head−head and head−drug interaction strength change. Changes in packing fraction have no effect on the internal structure of the micelles. However, changes in both head−head and head−solute interaction strength have significant effects on the micelle structure. Increasing the head−solute interaction strength causes the solute to be distributed throughout the core of the micelle more evenly. Increasing the head−head interaction strength pushes solute out of the micelle core toward the surface of the micelle.

We explained our results in terms of a model of solubilization proposed by Prud'homme and Kumar.[16] Their model describes the formation of an energy barrier to solute uptake around a micelle that gets stronger as more solute is loaded into the micelle. Although we do not calculate any energy barrier in our simulations directly, our results, especially those that show a significant amount of solute on the surface of the micelle, are consistent with the presence of this energy barrier. Furthermore, we infer that this energy barrier is stronger when the system variables are defined so that the copolymer forms micelles more easily (for example, at high packing fraction and high head−head interaction strength).

These results suggest ways that experimentalists could boost the encapsulation efficiency of their systems. Poor encapsulation efficiency can be counteracted by changing the head block used in the copolymer formulation. The poor release profile associated

with drugs remaining on the nanoparticle surface—a situation often encountered in the lab[4,5]—is likely caused by a copolymer headgroup that is too hydrophobic. Our research suggests that experimentalists could decrease drug surface binding and increase drug encapsulation by using a copolymer head block that is less hydrophobic than the one that causes drugs to get stuck on the micelle surface.

There are several possible ways to modify the copolymer so that the head block becomes more or less hydrophobic. A straightforward way to change the hydrophobicity of the copolymer is to change the length of the head block—a shorter head block would be less hydrophobic. The head block's hydrophobicity could also be modified by changing the chemical composition of the head block. A discussion of theoretical approaches for determining the hydrophobicity and the interaction parameters of copolymers and drugs in our previous paper.[17] These approaches do not preclude trial and error efforts to find the right copolymer; however, they do suggest ways to narrow the possible choices so that the trial and error process becomes more efficient.

■ ACKNOWLEDGMENT

This work was supported by the National Institutes of Health, USA, under Grant EB006006. We thank the Graduate Assistance in Areas of National Need (GAANN) Fellowship in Biotechnology for a portion of the funding for this research. We also thank Dr. Steven Smith, Dr. Andrew Schultz, and Dr. Zhengmin Li for their previous work in developing the simulation code used for this paper. Finally, we thank Dr. Robert Prud'homme for conversations that helped shape this work.

■ REFERENCES

(1) Alper, J. *Chemistry* **2005**, *2*, 23–27.
(2) Ferrari, M. *Nat. Rev. Cancer* **2005**, *5*, 161–171.
(3) Velluto, D.; Demurtas, D.; Hubbell, J. A. *Mol. Pharmaceutics* **2008**, *5*, 632–642.
(4) Fonseca, C.; Simoes, S.; Gaspar, R. *J. Controlled Release* **2002**, *83*, 273–286.
(5) Pan, J.; Liu, Y. T.; Feng, S. S. *Nanomedicine* **2010**, *5*, 347–360.
(6) Katsikogianni, G.; Avgoustakis, K. *J. Nanosci. Nanotechnol.* **2006**, *6*, 3080–3086.
(7) Pan, X. Y.; Yao, P.; Jiang, M. *J. Colloid Interface Sci.* **2007**, *315*, 456–463.
(8) Zhang, L. F.; Eisenberg, A. *Science* **1995**, *268*, 1728–1731.
(9) Alexandridis, P.; Holzwarth, J. F.; Hatton, T. A. *Macromolecules* **1994**, *27*, 2414–2425.
(10) Floriano, M. A.; Caponetti, E.; Panagiotopolous, A. Z. *Langmuir* **1999**, *15*, 3143–3151.
(11) Mackie, A. D.; Panagiotopolous, A. Z.; Szleifer, I. *Langmuir* **1997**, *13*, 5022–5031.
(12) Srinivas, G.; Discher, D. E.; Klein, M. L. *Nature Mater.* **2004**, *3*, 638–644.
(13) Mulqueen, M.; Blankschtein, D. *Langmuir* **1999**, *15*, 8832–8848.
(14) Larson, R. G. *J. Chem. Phys.* **1992**, *96*, 7904–7918.
(15) Shang, B. Z.; Wang, Z. W.; Larson, R. G. *J. Phys. Chem. B* **2008**, *112*, 2888–2900.
(16) Kumar, V.; Prud'homme, R. K. *J. Pharm. Sci.* **2008**, *97*, 4904–4915.
(17) Woodhead, J. L.; Hall, C. K. *Langmuir* **2010**, *26*, 15135–15141.
(18) Schultz, A. J.; Hall, C. K.; Genzer, J. *J. Chem. Phys.* **2002**, *17*, 10329–10338.
(19) Avgoustakis, K.; Beletsi, A.; Panagi, Z.; Klepetsanis, P.; Karydas, A. G.; Ithakissios, D. S. *J. Controlled Release* **2002**, *79*, 123–135.
(20) Dong, Y. C.; Feng, S. S. *Biomaterials* **2004**, *25*, 2843–2849.
(21) Marrink, S. J.; Tieleman, D. P.; Mark, A. E. *J. Phys. Chem. B* **2000**, *104*, 12165–12173.
(22) Scanu, L. F.; Gubbins, K. E.; Hall, C. K. *Langmuir* **2004**, *20*, 514–523.